Continuous detonation wave engine studies for space application

D. M. Davidenko, F. Jouot*, A. N. Kudryavtsev**, G. Dupré*, I. Gökalp*, E. Daniau***, and F. Falempin****
**ICARE – Institut de Combustion, Aérothermique, Réactivité et Environnement, CNRS*
1C avenue de la Recherche Scientifique, 45071 Orléans, France
***ITAM – Khristianovich Institute of Theoretical and Applied Mechanics,*
Russian Academy of Sciences, 630090 Novosibirsk, Russia
****MBDA France*
1 avenue Réaumur, 92358 Le Plessis Robinson, France

Abstract

Continuous Detonation Wave Rocket Engine (CDWRE) for space application is considered in the framework of French R&D and scientific research. 2D Euler simulations of a CDWRE combustion chamber have been performed to investigate the effect of geometrical and injection parameters on the internal process and combustion chamber performance. An experimental study on the detonation in a two-phase cryogenic flow is under progress. The paper presents an experimental installation intended for the investigation of liquid oxygen break-up and vaporization in a helium flow and of the detonation initiation and propagation in a spray of liquid oxygen/gaseous hydrogen.

1. Introduction

Theoretically, the rocket engine performance can be increased by the use of the detonation regime of combustion. Continuous Detonation Wave Rocket Engine (CDWRE) offers the potential of high specific impulse, high specific mass flow rate in a very compact package. The concept of CDWRE was proposed in the early 1960s by Russian scientist Voitsekhovskii[1] and experimentally proven for the first time at the Lavrentyev Institute of Hydrodynamics (LIH) of the Siberian Branch of the Russian Academy of Sciences. A detailed review of experimental investigations of this concept and its comparison with the conventional rocket engine can be found in recent publications[2,3].
After preliminary studies performed by MBDA in collaboration with LIH[4], French research activities on CDWRE for space applications are now conducted in the frame of the National Center of Technological Research (CNRT) "Propulsion du Futur", whose main contributors are MBDA France, Roxel France, and CNRS, with financial and technical support of the National Center of Space Research (CNES). These studies are aimed at the development of a full-scale engine that will be constructed and tested as a ground demonstrator within the next years[4].
From the CNRS side, scientific research related to CDWRE is conducted at LCD (Laboratoire de Combustion et Détonique)[5] and ICARE. At ICARE, research work is focused on two main subjects: numerical simulation of the continuous spin detonation in the combustion chamber and experimental investigation of the detonation initiation and propagation in a two-phase flow of gaseous hydrogen and liquid oxygen (GH_2-LO_2).

2. CDWRE operation

According to the CDWRE concept, the combustible mixture is continuously injected in the combustion chamber that can be shaped as a radial or a cylindrical duct. One or more transverse detonation waves move across the flow of combustible mixture. Due to the continuous injection, the mixture layer is restored between the successive detonation waves. In the moving frame related to a detonation front, the mean flow is steady.
For the propulsion applications, an annular cylindrical combustion chamber is the most appropriate configuration. It is schematically shown in Fig. 1. The mixture of fuel and oxidizer (1) is injected from the closed end (2) of the chamber through a ring slit or a large number of regularly arranged small holes. Transverse detonation waves (3) burn the layer of combustible gas (4). The azimuthal direction of detonation propagation is defined at the initiation and does not change if the detonation is stable. For a stable detonation propagation, the thickness of the fresh mixture layer h must be about 10-20 mm and the spatial period l between the fronts is typically (7±2) h depending on the

injection conditions[2]. Under these conditions, the detonation is close to the Chapman-Jouguet mode so the detonation frequency, f_D, (inverse time period between successive fronts) is of the order of 10 kHz . The detonation waves induce oblique shocks (5) in the burnt gas. The combustion products flow towards the duct open end (6) and then discharge from the chamber through a divergent nozzle (not shown in the scheme). Due to the combustion product expansion, a supersonic flow velocity can be achieved though the device has no geometrical throat.

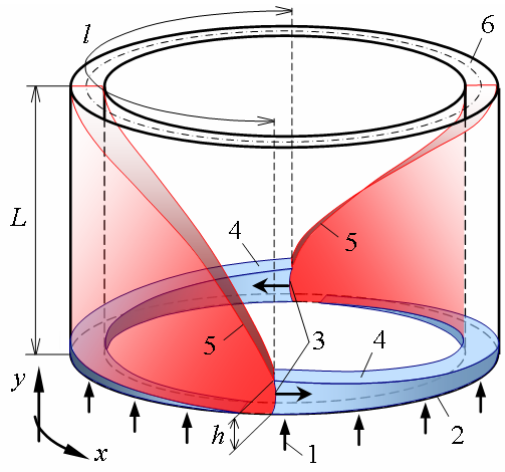

Figure 1: Schematic of a CDWRE combustion chamber.

CDWRE has several advantages with respect to the conventional liquid rocket engine (LRE):
– thermodynamically efficient internal process that can provide a higher specific impulse[4];
– lower heat loads on the wall (short combustion chamber, L = 100-200 mm, without geometrical throat);
– lower injection pressure with respect to the maximum pressure in the combustion chamber.

3. CDWRE demonstrator

Based on existing experience[2] and recent studies[4], related to the CDWRE startup and operation in a low-pressure environment, wall cooling, and structural materials, a demonstration engine has been designed by MBDA France. The layout of the CDWRE demonstrator is shown in Fig. 2. The annular duct of the combustion chamber has diameters of 350 mm and 280 mm corresponding to the external and internal walls.

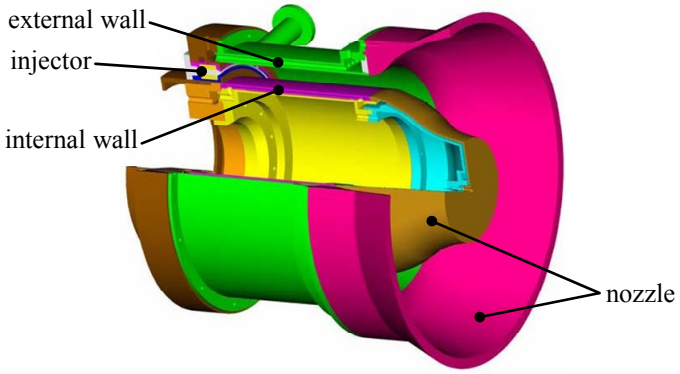

Figure 2: Layout of the CDWRE demonstrator.

The demonstrator will be able to operate with gaseous hydrogen (GH_2) and gaseous or liquid oxygen (GO_2 or LO_2). Thus different supply lines and injection walls will be needed. The injection pressure will be limited at 1-1.5 MPa and the total mass flow rate will be about 12-15 kg/s. The resulting mean pressure inside the combustion chamber is expected near 0.5 MPa, a value sufficient to deliver a thrust of several thousands of daN. The injection wall will be divided into 8 sectors to be able to control the local mass flow rate and to investigate the thrust vectoring effect with a diverging nozzle or with a center core nozzle (aerospike).
The test bench will be equipped with a complete weighing system providing measurements of thrust vector components and corresponding moments.

The engine structure will be modular and actively cooled. Thanks to its modularity, the demonstrator will be used as a non-flying workhorse allowing to address the following key points:
– effect of the injector configuration and injection conditions (GH_2/GO_2 or GH_2/LO_2);
– stability limits of the operation domain;
– viscous effects due to the high-speed flow (skin friction and heat fluxes);
– resistance of the fuel-cooled wall under the conditions of high-frequency mechanical and thermal shocks;
– effect of the asymmetric injection on the thrust vectoring with a full-size nozzle;
– vibration and acoustic operation environment.
Further, the modularity will allow to progressively replace all the engine components by flight-worthy ones. As a result, a flight-worthy demonstrator will be created and tested to assess the achievable performance when taking into account all the technology issues.

4. Computational study of CDWRE

Demonstrator tests will provide useful information for the CFD code validation. A reliable computational tool will be necessary to predict the engine performance under the conditions of significantly higher mass flow rates that will not be achievable on the test bench. Along with the preparation of demonstrator tests, numerical tools are developed and applied to the CDWRE simulation.
The numerical simulation of CDWRE in the full 3D configuration is rather expensive as a first approach. It is particularly true in the case of a parametric study. The problem can be simplified by assuming that the gap between the duct walls is small in comparison with their radii and the viscous effects on the walls can be neglected. Thus the flowfield variations in the radial direction are not considered and the duct is represented by a 2D planar geometry with periodicity conditions along the vertical boundaries as shown in Fig. 3.

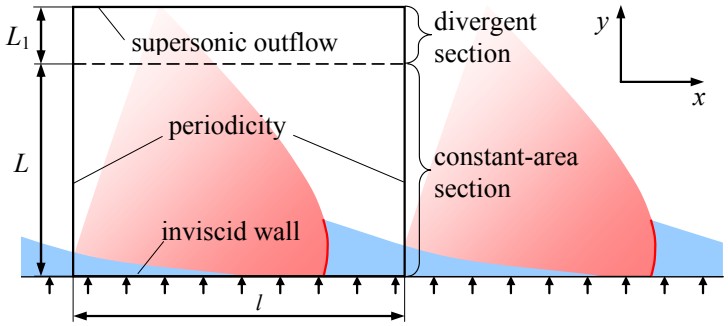

Figure 3: Schematic of the 2D computational domain.

The computational domain is rectangular, its x-wise size covers one spatial period l. Along y, the domain consists of a constant-area and a divergent sections whose lengths are denoted by L and L_1. In the present study, the domain dimensions vary within the following ranges: l = 50-100 mm, L = 10-100 mm. Within the divergent section of the duct, it is assumed that the duct cross-section area A linearly increases with y. The divergent section length L_1 = 10-20 mm and area ratio $A(L+L_1)/A(L)$ = 1.5-2 are arbitrarily chosen with the only purpose to ensure the supersonic outflow. Hence the combustion chamber operation does not depend on the external conditions.
The injection of stoichiometric mixture of H_2 and O_2 through the lower boundary (y = 0) is modeled as follows. The specified injection parameters are: the net area of injector throats A_j normalized by the overall area A_w of the injection wall, A_j/A_w = 0.1331, the total pressure P_{tj} = 1-6 MPa, and total temperature T_{tj} = 300 K. The area-specific mass flow rate $g_j(x) = G_j(x)/A_w$ depends on the wall pressure distribution $P_w(x)$. We suppose that the mixture is injected through an infinitely large number of uniformly distributed injectors so that g_j varies from zero at $P_w \geq P_{tj}$ to $g_{j\,max}$ at $P_w \leq P_{crj}$, where P_{crj} is the pressure at which the sonic injection condition is achieved. The injection conditions correspond to the demonstrator operation conditions however the range of P_{tj} variation is much larger.
The CDWRE combustion chamber is modeled using the two-dimensional Euler equations coupled with the mixture continuity equation, energy equation, and mass conservation equation for the chemical species. A high-resolution Euler code for a multispecies reactive flow is based on the shock-capturing, weighted essentially non-oscillatory (WENO) scheme of the fifth order, for the numerical flux approximation, and on a second-order semi-implicit additive Runge-Kutta scheme, for the time integration.
Perfectly reflecting or inviscid wall boundary conditions are imposed along the lower boundary. The mass, momentum and energy fluxes due to injection are evaluated every time step according to the local pressure in the first row of grid cells next to the wall. These fluxes are then added to the numerical fluxes calculated by the Euler

solver in the first cell row. The effect of duct expansion is modeled by introducing geometrical source terms into the governing equations. Simple extrapolation of conserved variables is utilized on the upper boundary.
The fluid is considered as a mixture of thermically perfect gases. A finite-rate chemical model is represented by a simple chemical kinetic mechanism[6], including 6 species (H_2, O_2, H_2O, H, O, and OH) and 7 reactions. The rate constants of the backward reactions have been refitted in a temperature range suitable for detonation simulations.
The thermochemical model and numerical code have been validated for some simple test problems such as constant-volume autoignition and 1D Zel'dovich-von Neumann-Döring detonations. The time and grid resolutions were chosen from 1D time-dependent simulations of freely propagating detonations to ensure correct predictions of the propagation velocity for the initial pressure varying from 0.1 MPa to 0.7 MPa. More details can be found in Ref. 7.
The simulated flowfield, in the moving reference frame related to the detonation front, is shown in Fig. 4 for the following case: P_{tj} = 3 MPa, $L = l$ = 100 mm. The colored fields display the variation of the Mach number, M_D, (Fig. 4a) and static temperature, T, (Fig. 4b) along with superimposed streamlines. Several characteristic zones are clearly depicted. The fresh mixture layer (1) is continuously growing from the lower boundary. In this layer, M_D is very high, from 5.5 up to 7. The detonation wave (2) is situated close to the right boundary. In front of the detonation wave, the mean static pressure and temperature are respectively 0.34 MPa and 259 K. The velocity of detonation propagation in the laboratory frame of reference, U_D, is of 2889 m/s, and the mean velocity of the detonation front with respect to the fresh mixture, D, is of 2922 m/s. Under these particular conditions, the propagation velocity of the ideal CJ detonation is D_{CJ} = 2915 m/s that means the simulated detonation is well matched the CJ regime. The maximum pressure and temperature obtained in the detonation wave are respectively 9.5 MPa and 4090 K.

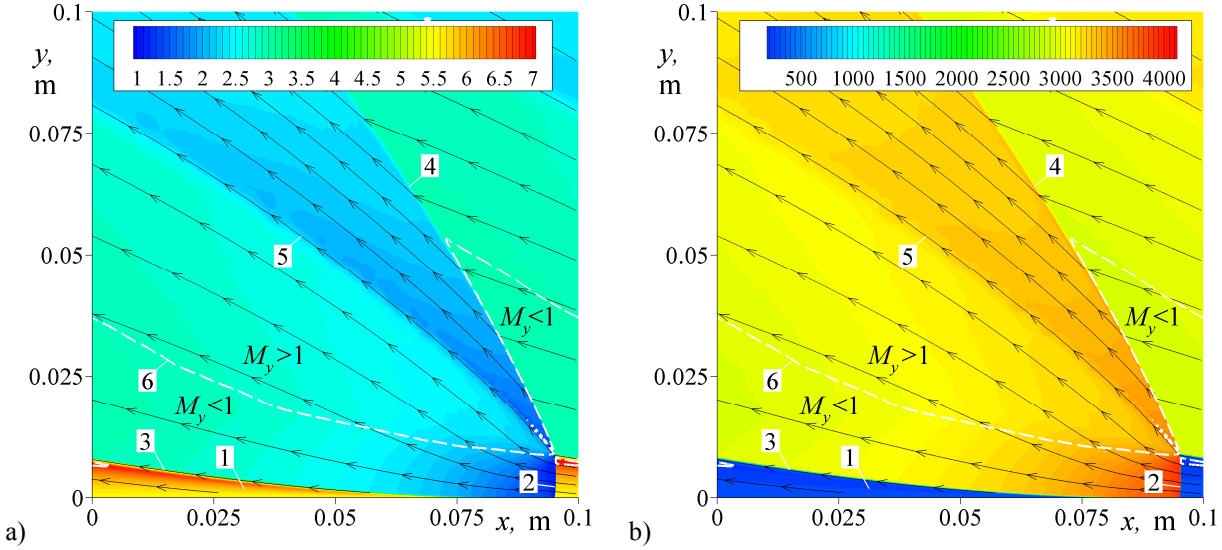

Figure 4: Flowfield structure in the combustion chamber corresponding to the moving reference frame: a) Mach number field, M_D; b) static temperature field, T (K).

Behind the detonation wave, the flow is subsonic within a very narrow zone. It rapidly accelerates to supersonic speeds due to a strong expansion of combustion products, which is clearly indicated by the diverging streamlines. The injection is suppressed over some distance behind the detonation wave because of a high pressure there. Two other waves are visible in Fig. 4 that originate from the point where the detonation wave meets the boundary (3) of the fresh mixture layer: a shock wave (4), which recompresses the flow of combustion products produced by the previous detonation, and a slip line or contact discontinuity (5), which separates the two streams of combustion products. A white dashed line (6) delimits the flowfield zones where the vertical velocity component is subsonic (M_y < 1) or supersonic (M_y > 1). One can notice that at y > 50 mm the flow is fully supersonic in the y-wise direction. In this case the duct expansion is not necessary to obtain a supersonic flow at the combustion chamber exit. The observed flow structure is qualitatively similar to that described in Ref. 2 and 3.
The time history of wall pressure variation $P_w(t)$ at a fixed point in the laboratory frame of reference is plotted in Fig. 5. It can be related to the instantaneous distribution $P_w(x)$ by the coordinate transformation $x = -U_D t$. The sharp peaks mark the detonation front. The detonation frequency is $f_D = U_D / l$ = 28.9 kHz. For the following consideration, we introduce the average wall pressure $\overline{P}_w = l^{-1}\int_0^l P_w(x)\,\mathrm{d}x$ and the average specific mass flow rate $\overline{g}_j = l^{-1}\int_0^l g_j(x)\,\mathrm{d}x$ as well as the wall pressure minimum $P_{w\,min} = \min[P_w(x)]$ and maximum $P_{w\,max} = \max[P_w(x)]$.
The effect of the injection pressure, P_{tj}, has been studied for fixed dimensions $L = l$ = 100 mm. The choice of P_{tj} provides that $\overline{g}_j$ corresponds to the experimental conditions[2] at P_{tj} = 1 MPa, whereas $\overline{g}_j$ is within the range of CDWE operating conditions[8] at P_{tj} = 3-6 MPa. From the simulation results, we find that P_{tj} can be considered as a

scaling factor for $\overline{g}_j$, $\overline{P}_w$, $P_{w\,min}$, and $P_{w\,max}$. In Fig. 6, one can see that $\overline{g}_j$ and $\overline{P}_w$ are linear functions of $P_{t\,j}$. For the chosen injector area ratio, A_j/A_w, and injectant total temperature, $T_{t\,j}$, $\overline{P}_w/P_{t\,j} = 0.444$ and $\overline{g}_j/P_{t\,j} = 170.8\times10^{-6}$ s/m. The wall pressure variation with respect to the average value can be estimated as follows: $P_{w\,min}/\overline{P}_w = 0.319$ and $P_{w\,max}/\overline{P}_w = 6.95$. The other characteristics are quite conservative with respect to $P_{t\,j}$: the overall increase of f_D is about 5 %; the mixture layer thickness, h, globally reduces by 9 %, from 0.095 l to 0.086 l; the combustion chamber specific impulse, I_{sp}, increases by 3.5 %, from 2795 m/s to 2933 m/s.

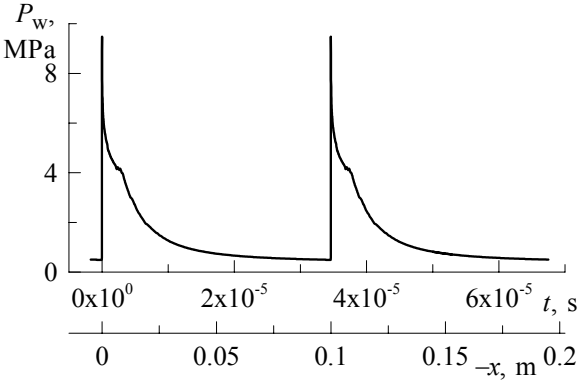

Figure 5: Temporal and spatial variation of the wall pressure.

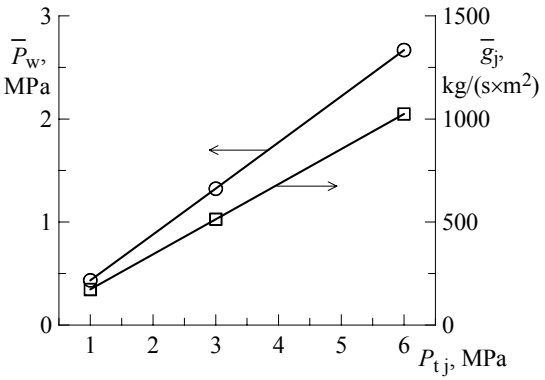

Figure 6: Average wall pressure and specific mass flow rate as functions of the injection total pressure.

To investigate the influence of the dimensions L and l, $P_{t\,j}$ is fixed at 3 MPa. The value of L is taken equal to 40 mm, 20 mm, and 10 mm at constant l = 100 mm. The detonation propagation is insensible to the variation of L until L is close to h. At $L \geq 40$ mm, the flow is not entirely supersonic at $y = L$. The subsonic-supersonic transition occurs at the very beginning of the divergent section. At L = 10 mm, P_w slightly diminishes and the top of the mixture layer appears in the divergent section ($h > L$). The detonation wave remains stable however I_{sp} globally decreases by 4.9 % because of growing nonuniformity of the flow at the combustion chamber exit ($y = L$).
Finally, the azimuthal period, l, is reduced to 75 mm and 50 mm keeping the other dimension constant, L = 40 mm. We find that l is a geometric scaling factor: f_D^{-1} and h are proportional to l. We also verified that the entire flowfield is self-similar if both the coordinates are normalized by l. The other characteristic quantities related to the injection ($\overline{g}_j$), detonation propagation (U_D), and wall pressure distribution ($\overline{P}_w$, $P_{w\,min}$, and $P_{w\,max}$) have no any noticeable change. Contrary to the reduction of L, a smaller period result in more homogeneous velocity profile at the combustion chamber exit.

5. Experimental study of the detonation in a two-phase cryogenic flow

In application to the space propulsion, CDWRE must operate with cryogenic liquid propellant. It is supposed that the engine will be fed with GH_2/LO_2. In this case, reliable initiation and stable propagation of a detonation in a two-phase cryogenic flow must be guaranteed. In the present experimental study, direct detonation initiation is one of the main subjects. Direct initiation means the detonation generation by an electrical energy release without any chemical sensitizer or mechanical device like Schelkin spiral implying a flame-to-detonation transition. Gaseous detonation initiation is determined by several parameters such as the equivalence ratio, mixture homogeneity, pressure, critical energy[9,10,11]. In application to the two-phase environment, liquid break-up and vaporization have to be added to the list of dominating factors. Many past experiments indicated that there is no principal difficulty associated with the detonation initiation and propagation in a fuel droplet spray suspended in a gaseous oxidizer[12,13,14]. In the present case, liquid oxidizer (LO_2) is atomized in a gaseous fuel (GH_2). In this configuration, typical for LRE, ignition and combustion at constant pressure has been well explored; on the other hand, experimental data on the detonation initiation and propagation are still limited.
In order to provide data necessary for the development of operational CDWRE, two experimental studies are under progress. The first one is focused on the atomization and vaporization of a nonreactive liquid jet in a gaseous flow. The second one deals with the detonation initiation and propagation in a reactive flow of GH_2/LO_2.

5.1 Liquid spray investigation

This part of the experimental work must yield data on the droplet size distribution in a two-phase flow under the

conditions that will be created later for the study of the detonation initiation and propagation. The injector design and injection conditions are different from those in a conventional LRE, thus the existing results from LRE studies cannot be directly applied.

The size distribution of liquid droplets will be explored along and across the flow. Knowing the droplet size distribution as a function of the distance from the injector and flow properties (Reynolds number *Re*, Weber number *We*, Ohnesorge number *Oh*, and gas-to-liquid momentum ratio *J*), it will be possible to describe the break-up and vaporization process of liquid oxidizer. In its turn, the detonation initiation and propagation in the two-phase reactive mixture will be strongly dependent on the liquid jet shattering and the following droplet break-up and vaporization. In this study, the Sauter mean diameter D_{32} is the main quantity to characterize the droplet size distribution as it indicates the mean volume-to-surface ratio. D_{32} is especially used in the case of spray combustion to indicate the importance of the surface exchange with respect to the droplet volume. Investigation of the surface transfer is relevant because the vaporization is a function of the square diameter of droplets.

The two-phase flow will be investigated in a semi-open tube 1 m long with a square cross section 50 mm × 50 mm. The tube walls are 10 mm thick. They are transparent to allow optical measurements inside the tube, which will be conducted with a He-Ne laser granulometer. A two-phase jet is created by an injector device installed in the center of the duct end wall. A flow of gaseous nitrogen, GN_2, is injected around the main jet to avoid the recirculation of two-phase flow near the end wall and the deposit of liquid on the internal walls. The walls are heated from outside to avoid water condensation from ambient atmosphere on the external surfaces.

The injector device is a coaxial aerodynamic atomizer schematically shown in Fig. 7. It is comprised of an annular conical channel for gaseous flow with equidistant walls (d_g = 0.72 mm) and a central cylindrical channel for liquid with a diameter d_l = 1.2 mm. The tip of the center nozzle is retracted by r = 0.85 mm with respect to the injector exit whose diameter is d_G = 4 mm.

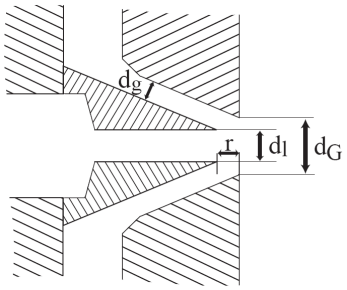

Figure 7: Coaxial atomizer for LO_2.

To model the two-phase GH_2/LO_2 flow in terms of break-up, vaporization, momentum and energy exchange conditions, it is planned to use gaseous helium, GHe, together with LO_2. The flow conditions will cover a range of Weber number *We* = 0-8000, a range of Reynolds number *Re* = 0-6000, and a range of momentum ratio *J* = 1-9 by respecting similarity with the GH_2/LO_2 reactive flow. The mass flow rate of LO_2 can cover a range from 1 g/s to 5 g/s while the corresponding mass flow rate of GH_2 varies from 0.3 g/s to 0.7 g/s. The injection pressure of LO_2 is relatively low providing a pressure difference ΔP = 0.1 MPa but there is a possibility to extend it to 1.5 MPa. The gaseous flow can be pressurized from 0.5 MPa to 5 MPa.

Preliminary tests have been performed to calibrate the injector device. An unconfined two-phase jet of water atomized by air flow was studied with the granulometer. The droplets size evolution along the jet is shown in Fig. 8 for various injection conditions in terms of *We* and *J*.

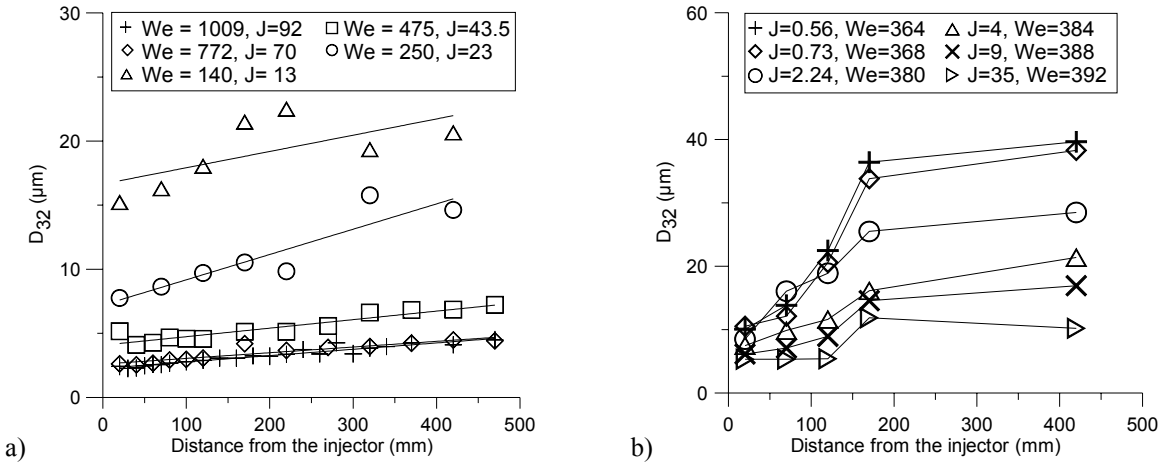

Figure 8: Effect of the Weber number (a) and momentum ratio (b) on the longitudinal distributions of Sauter mean diameter in the water-air two-phase jet.

The data presented in Fig. 8a were obtained for a range of air velocity from 37 m/s to 300 m/s and for a range of water velocity from 1 m/s to 9 m/s. In the experiments corresponding to Fig. 8b, the air velocity was kept constant at 180 m/s while the water velocity varied between 1 m/s and 8 m/s. The observed behaviour of D_{32} is typical: the

droplet size becomes smaller as *We* and *J* increase. Figure 8b shows that the influence of *J* on D_{32} is more important in the far-field than in the near-field.

5.2 Experimental setup for the two-phase detonation

By this study, we expect to characterize conditions for the detonation initiation and propagation in a two-phase cryogenic environment depending on the droplet size distribution, global equivalence ratio, initial pressure, and initiation energy.
The experimental setup for the study of two-phase detonations is presented in Fig. 9. The injector device and the rectangular tube (not shown in the scheme) are of the same geometry as for the liquid spray study. The tube consists of 4 welded plates of stainless steel. A moving cap is installed opposite the open end of the tube to control the exit area thus enabling experiments under pressure.

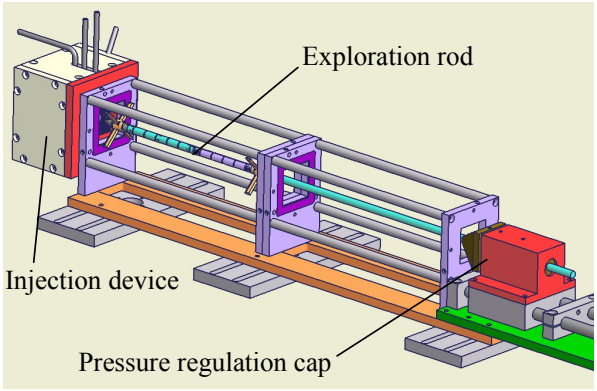

Figure 9: Experimental setup for the two-phase detonation.

The injection conditions will be similar to those considered for the spray study in terms of *We*, *Re*, and *J*. At the beginning of a test run, a two-phase jet is created by feeding GHe/LO_2 to the injector and GN_2 around the jet. When the operation is stable, GHe is replaced with GH_2. The equivalence ratio of the reactive mixture is globally determined with flow meters. The detonation is initiated when the tube is purged with reactive mixture.
Direct initiation will be attempted by a spark created between two electrodes. The electrical discharger can be installed in different locations along the tube. Changing location allows investigating how different stages of break-up and vaporization of the cryogenic spray (from the liquid core to the purely gaseous mixture) affect the conditions of detonation initiation. The electrical energy will be stored in condensers. Amount of released energy will cover a range from few Joules to several hundreds of Joules in order to estimate the minimum energy required for the direct initiation of detonation.
Litchfied et al.[11] determined minimum energy required for the direct detonation initiation in gaseous hydrogen-oxygen mixtures: around 10 J for exploding wire and about 100 J for spark ignition. In the present study, spark ignition is preferred to the exploding wire technique because it provides a faster deposit of energy, which is of primary importance for direct initiation. The energy transmitted from the spark to the mixture is a dominant parameter but difficult to quantify.
To study the detonation propagation in the core flow, an exploration rod will be introduced in the tube. It will allow measurements of pressure and detonation cell size. The arrangement of the exploration rod is presented in Figures 9 and 10.

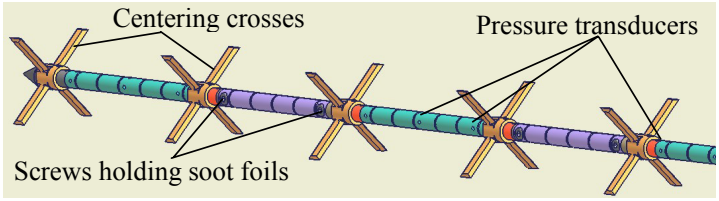

Figure 10: Exploration rod layout.

The rod is divided into alternate measurement sections. Within one section, there is a number of pressure transducers mounted flush on the rod surface. Another section have a soot foil rolled around the rod. Several crosses are installed between the measurement sections to center the rod inside the tube. Fast pressure transducers will give information

on the detonation wave velocity whereas the soot foils will record the detonation cellular structure. This information will be necessary to assess whether the detonation reaches the Chapman-Jouguet mode and what is the detonability of reactive mixture.

6. Conclusion

In France, R&D and scientific studies are conducted on the space propulsion application of the CDWRE concept. A CDWRE demonstrator operating with GH_2/GO_2 or GH_2/LO_2 is under development. It will be exploited within the next years to validate technological solutions for the future operational engine.
Along with the demonstrator preparation, numerical simulations of the CDWRE internal process are conducted. A parametric study has been performed for a simplified 2D configuration. The flowfield structure in the combustion chamber has been investigated and two scaling factors (P_{tj} and l) have been identified.
In parallel, an experimental work is under progress. An experimental installation is being prepared to start experiments this year, first, to characterize the break-up and vaporization in a GHe/LO_2 flow, and second, to study the conditions of detonation initiation and propagation in a GH_2/LO_2 flow.

Acknowledgments

The authors thank MBDA France and CNES for the financial support of this work. Computational resources for the numerical simulations have been provided by the research federation EPEE of CNRS and the University of Orléans.

References

[1] Voitsekhovskii, B.V. Stationary spin detonation, *Soviet Journal of Applied Mechanics and Technical Physics*, 3:157-164, May-June 1960.
[2] Bykovskii, F.A., Zhdan, S.A., and Vedernikov, E.F. Continuous spin detonations, *Journal of Propulsion and Power*, 22:1204-1216, 2006.
[3] Zhdan, S.A., Mardashev, A.M., and Mitrofanov, V.V. Calculation of the flow of spin detonation in an annular chamber, *Fizika Goreniya i Vzryva*, 26:91-95, 1990.
[4] Falempin, F., Daniau, E., Getin, N., Bykovskii, F. A., and Zhdan, S. Toward a continuous detonation wave rocket engine demonstrator, AIAA-2006-7956, *14th AIAA/AHI Space Planes and Hypersonic Systems and Technologies Conference*, Canberra, 6-9 November 2006.
[5] Canteins, G. Étude de la détonation continue rotative – Application à la propulsion, PhD thesis, Université de Poitiers, École Nationale Supérieure de Mécanique et d'Aérothermique, November 2006.
[6] D.M. Davidenko, I. Gökalp, E. Dufour, P. Magre, Systematic numerical study of the supersonic combustion in an experimental combustion chamber, AIAA-2006-7913, *14th AIAA/AHI Space Planes and Hypersonic Systems and Technologies Conference*, Canberra, 6-9 November 2006.
[7] Davidenko, D. M., Gökalp, I., and Kudryavtsev, A. N. Numerical modeling of the rotating detonation in an annular combustion chamber fed with hydrogen-oxygen mixture, *3rd European Combustion Meeting ECM 2007*, Crete, 11-13 April 2007.
[8] Daniau, E., Falempin, F., and Zhdan, S. Pulsed and rotating detonation propulsion systems: first step toward operational engines, AIAA-2005-3233, *13th AIAA/CIRA Space Planes and Hypersonic Systems and Technologies Conference*, Capua, 16-20 May 2005.
[9] Knystautas, R. and Lee, J. H. On the effective energy for direct initiation of gaseous detonations, *Combustion and Flame*, 27: 221-228, 1976.
[10] Zitoun, R., Desbordes, D., Guerraud, D., and Deshaies B. Direct initiation of detonation in cryogenic gaseous H_2-O_2 mixtures, *Shock Waves*, 4: 331-337, 1995.
[11] Litchfield, E. L. Hay, M. H., and Forshey, D. R. Direct electrical initiation of freely expanding gaseous detonation waves, *9th Symposium (International) on Combustion*, The Combustion Institute, pages 282-286, 1963.
[12] Webber, W. T. Spray combustion in the presence of a travelling wave, *8th Symposium (International) on Combustion*, The Combustion Institute, pages 1129-1140, 1962.
[13] Ragland, K. W., Dabora, E. K., and Nicholls J.A. Observed structure of spray detonations, *Physics of fluids*, 11:2377-2388, 1968.
[14] Frolov, S. M., Basevich, V. Y., Aksenov, V.S., and Polikhov S.A. Detonation initiation in liquid fuel sprays by successive electric discharges, *Doklady Physical Chemistry*, 392(2):39-41, 2004.

A revised version of this article is availabe here.